Dalton Transactions

PAPER

View Article Online
View Journal | View Issue

Published on 17 February 2015. Downloaded by Seton Hall University on 05/04/2015 14:27:06.

Cite this: *Dalton Trans.*, 2015, **44**, 5379

Molten salt synthesis, visible and near-IR region spectral properties of europium or neodymium doped $CoNb_2O_6$ columbite niobate

Mete Kaan Ekmekçi,*[a] Murat Erdem[b] and Ali Sadi Başak*[a]

Received 29th September 2014,
Accepted 4th February 2015

DOI: 10.1039/c4dt03001j

www.rsc.org/dalton

Pure Nd^{3+}- or Eu^{3+}-doped $CoNb_2O_6$ powders have been prepared by a molten salt synthesis method using a Li_2SO_4–Na_2SO_4 or NaCl–KCl salt mixture as a flux at relatively low temperatures as compared to the solid state reaction method. X-ray diffraction patterns of pure $CoNb_2O_6$ samples indicated an orthorhombic single phase. For Eu^{3+}-doped $CoNb_2O_6$ samples, the luminescence of Eu^{3+} was observed at 615 nm as red emission while the Nd^{3+} doped sample showed a typical emission at 1064 nm varying with the Eu^{3+} or Nd^{3+} doping concentrations. These luminescence characteristics of the doped samples may be attributed to the energy transfer between rare earth ions and CoO_6 octahedral groups in the columbite structure.

1. Introduction

Columbite structured metal niobate compounds are good candidates as a host matrix for rare earth ions in terms of many optical and photonic applications. Columbite binary niobate ceramics with the general formula MNb_2O_6 (M = Co, Cd, Ni, Mg, Cu, Zn, Mn *etc.*) have an orthorhombic crystal structure and a space group *Pbcn* = 60. In the MNb_2O_6 columbite structure, there are two kinds of octahedra MO_6 and NbO_6. These octahedra constitute the columbite structure by sharing edges and corners in the order of regular zig-zag chains (MO_6 chain–NbO_6 chain–NbO_6 chain).[1] There are a few studies on the luminescent properties of rare earth doped columbite transition metal niobate compounds in the literature.[2–37]

$CoNb_2O_6$ is a very interesting material due to its ease of synthesis in different ways[8–10] and has quasi-one-dimensional Ising magnetic properties with a Neel temperature of 2.95 K.[11] $CoNb_2O_6$ is a key material to be used in the synthesis of Pb$(Co_{1/3}Nb_{2/3})O_3$ lead base relaxer ferroelectrics.[12] The dielectric properties of $CoNb_2O_6$ were investigated by Maeda *et al.*[13] They reported that $CoNb_2O_6$ has poor properties ($Q \times f$ = 6800 and 20) due to its large porosity. A molten salt synthesis method is not reported for the preparation of undoped and rare earth ion doped $CoNb_2O_6$ in the literature. It is one of the most practicable and versatile methods which allows lower calcination temperature and dwell time in the synthesis.

When compared to traditional conventional solid state synthesis methods such as a mixed oxide route, single phase $CoNb_2O_6$ obtainable after >2 h at 1050–1100 °C (ref. 14, 15) and heating at 1370 K for 30 h with intermediate grinding in the literature, where the molten salt synthesis method suggests a much lower calcination temperature such as 800 °C in our study.[16] Moreover, in the temperature range of 700–900 °C, the formation of intermediate phase $Co_4Nb_2O_9$ and residual Nb_2O_5 has been avoided by the molten salt method.[17–35]

There are three main steps in the molten salt synthesis method: (i) mixing of oxides and salt(s) mechanically as reactants and flux(es) respectively; (ii) homogenization of the reactants in molten salt(s) reaction media; (iii) heat treatment for nucleation and improvement of the desired phase. Besides, molten salt or salt mixtures can be easily removed from the main compound by washing with distilled water after the synthesis.[18–20]

Neodymium (Nd^{3+}) ion doped crystals and glasses are widely used as solid-state laser materials in photonic applications.[21–36] From the $^4F_{3/2}$ upper laser level of the $4f^3$ electrons of the Nd^{3+} ion transitions occur at all levels of the ^4I_J manifold with J = 15/2 (transition wavelength $\lambda \sim 1.8$ μm), J = 13/2 ($\lambda \sim 1.32$ μm), J = 11/2 ($\lambda \sim 1.06$ μm) and J = 9/2 ($\lambda \sim$ 0.88 μm, ground state).

The Nd^{3+} doped columbite niobate crystals generally operate in the $^4F_{3/2} \rightarrow {}^4I_{11/2}$ transition emitting around 1.06 μm where they could be candidates as solid-state lasers.[6]

Europium (Eu^{3+}) ions have been known as an excellent red activator in many phosphorus materials because of the intra-4f-shell transitions between the $^5D_0 \rightarrow {}^7F_J$ (J = 0, 1, 2, 3, 4) levels, such as $NaSr_2Nb_5O_{15}$:Eu^{3+}, $KNbO_3$:Eu^{3+}, *etc.*[27,28]

[a]*Marmara University, Art and Science Faculty, Chemistry Department, Inorganic Chemistry Division, Istanbul, Turkey. E-mail: asbasak@marmara.edu.tr, mekmekci@marmara.edu.tr*
[b]*Marmara University, Art and Science Faculty, Physics Department, , Istanbul, Turkey*

Published on 17 February 2015. Downloaded by Seton Hall University on 05/04/2015 14:27:06.

If a rare earth ion invades a site that has inversion symmetry (centrosymmetric) in the crystal lattice, band passes between the $4f^n$ configurations are electric dipole forbidden while magnetic dipole pass occurs between $^5D_0 \rightarrow {}^7F_1$ (~590 nm) energetic bands showing orange emission in the case of no inversion symmetry (non-centrosymmetric) in the rare earth ion (Eu^{3+}) site.[28]

In this paper, Eu^{3+}- or Nd^{3+}-doped $CoNb_2O_6$ (CoN) was synthesized by molten salt synthesis and was characterized by XRD and SEM-EDS analyses; spectral characterization of doped powders in Vis (400 nm–700 nm) and near-IR spectral regions (850 nm–1150 nm) has been investigated. The influence of the Eu^{3+} or Nd^{3+} concentration on the luminescence properties was also studied.

To our knowledge this is the first report on the molten salt synthesis and structural and spectroscopic characterization of this promising host material.

2. Experimental

Undoped Eu^{3+} or Nd^{3+} doped (0.5, 3.0 and 6.0 mol%) $CoNb_2O_6$ columbite crystals were synthesized *via* the molten salt route by mixing $Co(NO_3)_2{\cdot}6H_2O$, Nb_2O_5, Eu_2O_3 or Nd_2O_3 in 2 : 1 salt/oxide molar ratio and a Li_2SO_4–Na_2SO_4 salt mixture in 0.635/0.365 and a NaCl–KCl salt mixture in 1 : 1 molar ratio except for the synthesis of doped powders as a flux separately, and grinded well in terms of providing homogeneity. After that, sufficient amount of the mixture settled in the alumina crucible and calcined at 800 °C for 4 hours. After the heat treatment, for the purpose of eliminating the ionic salts from the main product, mixtures were washed with ultra-pure water and vacuum filtered several times. The presence of such ions in the filtrate was checked by using qualitative reactions. Because Nd^{3+} and Eu^{3+} ions substitute Co^{2+} due to their similarity in ionic radii, the single phase of the doped columbite structure was achieved by an appropriate calcination temperature. An examination of crystal quality (presence of microdefects, inclusion of secondary phases, *etc.*) was done by scanning electron microscopy (SEM) and electron diffraction spectroscopy (EDS), and X-ray diffraction patterns of powders obtained using a Rigaku Rotaflex model RU200B using Cu Kα radiation (λ = 1.546 Å) with a step scan of 0.02° in the 2θ range of 10–70°. Luminescence spectra of the compounds were recorded using a Scinco, Floromaster FS/2 model fluorescence spectrophotometer in the wavelength range of 200–900 nm. The luminescence spectra of the powders in the near infrared spectral region were recorded using a diode laser (Apollo Instruments-S30-808-6) with a wavelength of 805.2 nm to excite the powders from the ground state ($^4I_{9/2}$) to the higher $^4F_{5/2}$ excited state of Nd^{3+} ions. The luminescence from the powders was focused onto a Monochromator (Spectra SP-2-500i Model 2051) and detected by using an InGaAs (ID-441-C model) detector. All the measurements were carried out at room temperature.

3. Results and discussion

3.1. Structural and spectroscopic characterization

3.1.1. X-ray diffraction analysis results. In the synthesis of pure $CoNb_2O_6$ powders, different heat treatment temperatures and NaCl/KCl and Li_2SO_4/Na_2SO_4 salt systems have been used as reaction media to determine the optimum synthesis parameters.

Fig. 1 shows the XRD patterns of $CoNb_2O_6$ powders calcined at temperatures between 700 and 1100 °C by using NaCl/KCl (salt : salt = 1 : 1 and salt : oxide = 2 : 1 molar ratios) for a dwell time of 4 hours. Because $CoNb_2O_6$ starts to form at 600 °C the calcination temperature has been set as 700 °C which is just above the formation temperature.[29] Results of the XRD analysis of $CoNb_2O_6$ powders synthesized at 700 °C for 4 hours by using a NaCl–KCl salt mixture as a reaction medium showed that the single phased orthorhombic $CoNb_2O_6$ (JCPDS file no. 38-1428) has been successfully obtained by the molten salt method. It can be found in the $CoNb_2O_6$ phase (JCPDS file no. 32-0304) at only 700 °C calcined temperature. The samples exhibited a single phase and all of the peaks were found to be in the orthorhombic $CoNb_2O_6$ phase at related temperatures. A minor phase (Co_3O_4) (JCPDS file no. 18-0258) which was mentioned by other researchers at 700 °C calcined temperature was eliminated. Rising of the calcination temperature from 700 to 750 °C has afforded small amounts of Nb_2O_5 (JCPDS Card no. 27-1003) minor phase. When the temperature reached 800 °C, the quantity of Nb_2O_5 increased. Moreover, the $NaNbO_3$ (JCPDS Card no: 33-1270) interphase has also occurred and the quantity of the $CoNb_2O_6$ phase has reduced. By increasing the temperature to 900 °C, the quantity of the $NaNbO_3$ interphase has increased (Tables 1 and 2).

Because of the Nb_2O_5 and $NaNbO_3$ minor phase formation, a single phased $CoNb_2O_6$ structure has not been successfully obtained for all which annealed at 1000 and 1100 °C respectively. All these results show that the calcination temperature of 700 °C and the NaCl/KCl salt : salt system are the most suitable for the synthesis of the single phase columbite $CoNb_2O_6$.

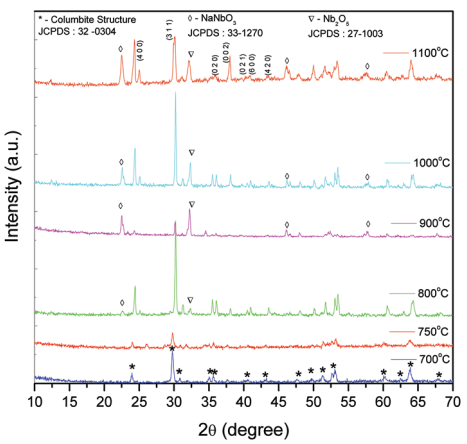

Fig. 1 XRD patterns of the powders with a NaCl/KCl salt mixture calcined between 700 and 1100 °C for 4 h.

 This journal is © The Royal Society of Chemistry 2015

Published on 17 February 2015. Downloaded by Seton Hall University on 05/04/2015 14:27:06.

Table 1 Synthesis parameters of undoped $CoNb_2O_6$ powders and their phase compositions

Compound	Salt system and salt/salt molar ratio	Salt/oxide weight ratio	Heat treatment	Phases
$CoNb_2O_6$	NaCl/KCl	01 : 01	700, 4 h	$CoNb_2O_6$
$CoNb_2O_6$	NaCl/KCl	01 : 01	750, 4 h	$CoNb_2O_6$, Nb_2O_5
$CoNb_2O_6$	NaCl/KCl	01 : 01	800, 4 h	$CoNb_2O_6$, Nb_2O_5, $NaNbO_3$
$CoNb_2O_6$	NaCl/KCl	01 : 01	900, 4 h	$CoNb_2O_6$, Nb_2O_5, $NaNbO_3$
$CoNb_2O_6$	NaCl/KCl	01 : 01	1000, 4 h	$CoNb_2O_6$, Nb_2O_5, $NaNbO_3$
$CoNb_2O_6$	NaCl/KCl	01 : 01	1100, 4 h	$CoNb_2O_6$, Nb_2O_5, $NaNbO_3$
$CoNb_2O_6$	Li_2SO_4/Na_2SO_4	02 : 01	700, 4 h	$CoNb_2O_6$, Nb_2O_5
$CoNb_2O_6$	Li_2SO_4/Na_2SO_4	02 : 01	800, 4 h	$CoNb_2O_6$
$CoNb_2O_6$	Li_2SO_4/Na_2SO_4	02 : 01	900, 4 h	$CoNb_2O_6$, Nb_2O_5, $NaNbO_3$
$CoNb_2O_6$	Li_2SO_4/Na_2SO_4	02 : 01	950, 4 h	$CoNb_2O_6$, $NaNb_2O_5$
$CoNb_2O_6$	Li_2SO_4/Na_2SO_4	02 : 01	1000, 4 h	$CoNb_2O_6$, Nb_2O_5, $NaNbO_3$

Table 2 Synthesis parameters of Eu^{3+} and Nd^{3+}doped $CoNb_2O_6$ powders and their phase compositions

Compound	Salt system and salt/salt molar ratio	Salt/oxide weight ratio	Heat treatment	Phases
0.5 mol% Eu^{3+} doped $CoNb_2O_6$	Li_2SO_4/Na_2SO_4 0.635/0.365	02 : 01	800 °C, 4 h	$CoNb_2O_6$
3.0 mol% Eu^{3+} doped $CoNb_2O_6$	Li_2SO_4/Na_2SO_4 0.635/0.365	02 : 01	800 °C, 4 h	$CoNb_2O_6$, $EuNbO_4$
6.0 mol% Eu^{3+} doped $CoNb_2O_6$	Li_2SO_4/Na_2SO_4 0.635/0.365	02 : 01	800 °C, 4 h	$CoNb_2O_6$, $EuNbO_4$
0.5 mol% Eu^{3+} doped $CoNb_2O_6$	Li_2SO_4/Na_2SO_4 0.635/0.365	02 : 01	800 °C, 4 h	$CoNb_2O_6$

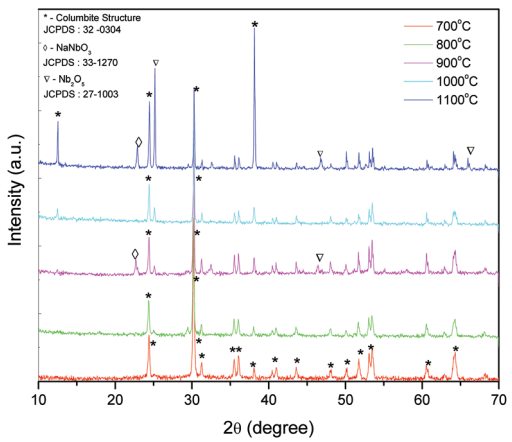

Fig. 2 XRD patterns of the powders with an Li_2SO_4/Na_2SO_4 salt mixture calcined at 800 °C for 4 hours.

Fig. 2 shows the XRD patterns of $CoNb_2O_6$ powders synthesized by using the Li_2SO_4–Na_2SO_4 salt system annealed at different temperatures of 700–1100 °C for 4 h. A large amount of $CoNb_2O_6$ has been obtained at 700 °C but little amount of Nb_2O_5 (JCPDS Card no: 27-1003) minor phase occurred. For the synthesis of $CoNb_2O_6$ at 800 °C, a pure orthorhombic $CoNb_2O_6$ (JCPDS Card no. 32-304) single phase has been observed. No other interphases were seen for this sample. Increasing of the calcination temperature to 900 °C caused the deviation from the single phased structure and minor phases such as Nb_2O_5 and $NaNbO_3$ occurred. Rising of the temperature to 950 °C has caused an increase in the quantity of the $NaNbO_3$ minor phase. Finally, the calcination temperature of 1000 °C has shown an increase in the phase quantity of both Nb_2O_5 and $NaNbO_3$.

The intensity of the XRD peaks was found to increase with the increasing heat treatment temperature. This is due to an increase of energy given to samples, which in turn will increase the probability of crystallization to take place. The heat treatment will always enhance crystallinity and at certain temperature the phase transition will occur. An XRD spectrum is shown in Fig. 1 to compare the crystallinity of the samples synthesized at different temperatures. The sample forms the major $CoNb_2O_6$ crystalline phase on its heat treatment by the following reaction: $Co(NO_3)_2{\cdot}6H_2O + Nb_2O_5 \rightarrow CoNb_2O_6 + 2NO_2 + 6H_2O$. In addition, traces of the $NaNbO_3$ crystalline phase are formed by the following reaction: $6NaCl + 3Nb_2O_5 + 3/2\ O_2 \rightarrow 6NaNbO_3 + 3Cl_2$ and Nb_2O_5 which remains as the unreacted phase. The volume fraction of the two phases ($NaNbO_3$ and Nb_2O_5) increases as compared to the volume fraction of the $CoNb_2O_6$ phase with increasing heat treatment temperature. It is because of the fact that the activation energy for crystallization of the two phases $NaNbO_3$ and Nb_2O_5 is higher than the activation energy of the major phase.[30]

All these results indicate that the calcination temperature of 800 °C and the Li_2SO_4–Na_2SO_4 salt : salt system and the calcination temperature of 700 °C and the NaCl–KCl salt : salt system are most suitable for the synthesis of the single phase columbite $CoNb_2O_6$. 800 °C and the Li_2SO_4–Na_2SO_4 salt : salt system also have been used in the synthesis of Nd doped powders preferably.

Published on 17 February 2015. Downloaded by Seton Hall University on 05/04/2015 14:27:06.

In the synthesis of 0.5, 3.0, 6.0 mol% Nd-doped $CoNb_2O_6$ powders *via* the molten salt synthesis route by using the same appropriate salt/oxide molar ratio and the same ambient calcination conditions, the single phase $CoNb_2O_6$ (JCPDS Card no: 32-304) formed at 0.5 mole doping concentrations. When the doping concentration reached 3.0 and 6.0 mol% concentrations, the $NdNbO_4$ (JCPDS Card no. 32-380) interphase has been observed.

Fig. 3 shows the XRD patterns of Nd^{3+} doped $CoNb_2O_6$ powders synthesized by molten salt synthesis at 800 °C for 4 hours. Synthesis of undoped and 0.5, 3.0, 6.0 mol% Nd-doped $CoNb_2O_6$ powders *via* the molten salt route by using the salt/oxide molar ratio of 1 : 1 gave the orthorhombic single phase $CoNb_2O_6$ (JCPDS Card no. 38-1428). No other second phases were observed in the XRD. A remarkable shift to lower angles was observed for the high Nd^{3+} concentrations. These peak shifts indicate the presence of strains in the doped host lattices due to the doping of the Nd^{3+} cation which has slightly larger ionic radii than Co^{2+} (1.123 Å for Nd^{3+} and 0.88 Å for Co^{2+}).[31]

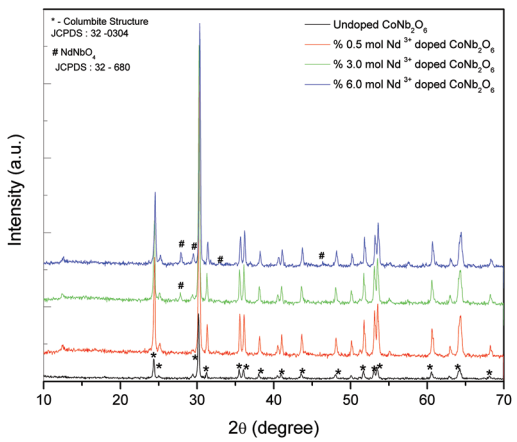

Fig. 3 XRD patterns of the 0.5, 3 and 6 mol% Nd doped powders with a Li_2SO_4/Na_2SO_4 salt mixture calcined at 800 °C for 4 hours.

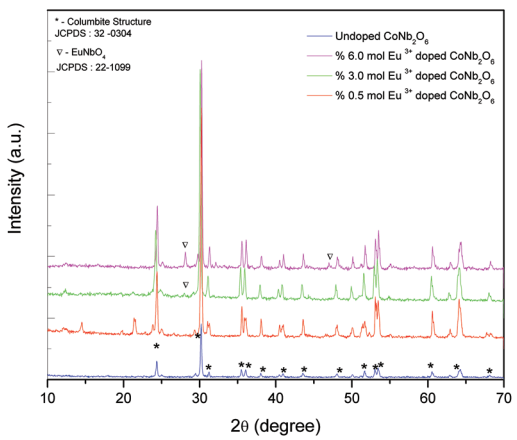

Fig. 4 XRD patterns of the 0.5, 3.0 and 6.0 mol% Eu doped powders with a Li_2SO_4/Na_2SO_4 salt mixture calcined at 800 °C for 4 hours.

Fig. 4 shows the XRD patterns of undoped, 0.5, 3.0 and 6.0 mol% Eu doped $CoNb_2O_6$ powders synthesized by molten salt synthesis at 800 °C for 4 hours. Synthesis of 0.5, 3.0, 6 mol% Nd-doped $CoNb_2O_6$ powders *via* the molten salt route by using the Li_2SO_4/Na_2SO_4 salt/oxide salt system with a molar ratio of 2 : 1 gave the orthorhombic single phase only for 0.5 mol% Eu^{3+} doped CoNb2O6 (JCPDS Card no. 32-0304). Besides, increasing of the Eu^{3+} concentration from 0.5 to 3.0 mol% resulted in the $EuNbO_4$ (JCPDS Card no: 22-1099) secondary phase and the amount of this phase has increased by increasing the Eu^{3+} concentration from 3.0 to 6.0 mol% in the XRD. The possible reason for this is that the ionic ratio of the Eu^{3+} ion (1.123 Å) is greater than that of the Co^{2+} ion (0.88 Å) and so, lack of insertion and incomplete insolubility of dopant in the host may lead to the secondary $EuNbO_4$ phase. Moreover, the activation energy for crystallization of the $EuNbO_4$ phase is higher than the activation energy of the major phase is considered.[30]

3.1.2. Scanning electron microscopy (SEM) analysis results. The surface morphology and microstructure of powders were examined using a scanning electron microscope (SEM; Jeol JSM 5910LV) equipped with an EDS (Oxford Instruments Inca X-Sight 7274).

The SEM images of the undoped, 0.5 and 6.0 mol% Nd doped $CoNb_2O_6$ powders are illustrated in Fig. 5, 6 and 7 respectively. As can be seen, the SEM micrographs of the undoped and 0.5 mol% Nd doped samples in Fig. 5 and 6, respectively show single phase structures with an irregular round-like morphology. EDS analysis from the particles signed with number 1 in the SEM image also indicated that the atomic weight ratio of the elements were in agreement with the theoretical compositions of $CoNb_2O_6$.

It is also seen from Fig. 6 that increasing of the dopant concentration to 6.0 mol% leads to unexpected $NdNbO_4$ minor phase formation. Moreover, EDS measurements also support the SEM result.

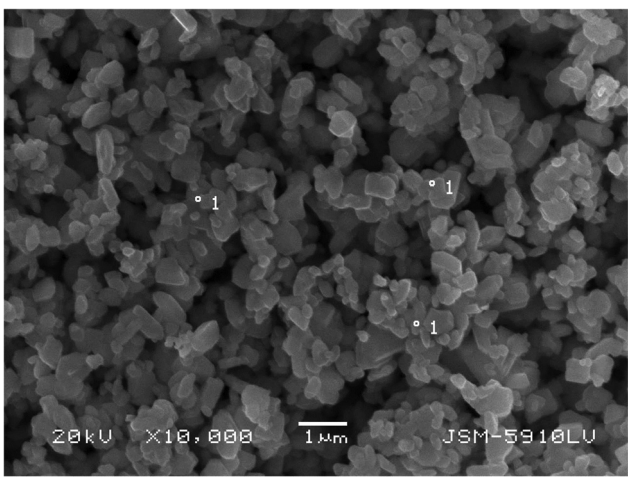

Fig. 5 The SEM picture of the undoped $CoNb_2O_6$ columbite powders calcined at 800 °C. Point (1) indicates the single $CoNb_2O_6$ phase.

This journal is © The Royal Society of Chemistry 2015

Published on 17 February 2015. Downloaded by Seton Hall University on 05/04/2015 14:27:06.

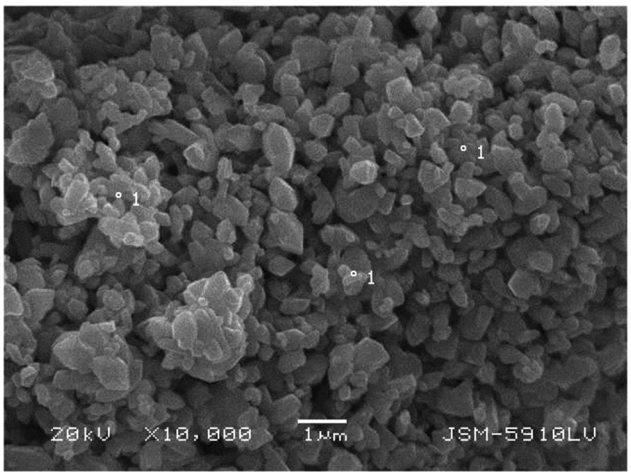

Fig. 6 The SEM picture of the 0.5 mol% Nd doped $CoNb_2O_6$ columbite powders calcined at 800 °C for 4 hours. Point (1) indicates the single $CoNb_2O_6$ phase.

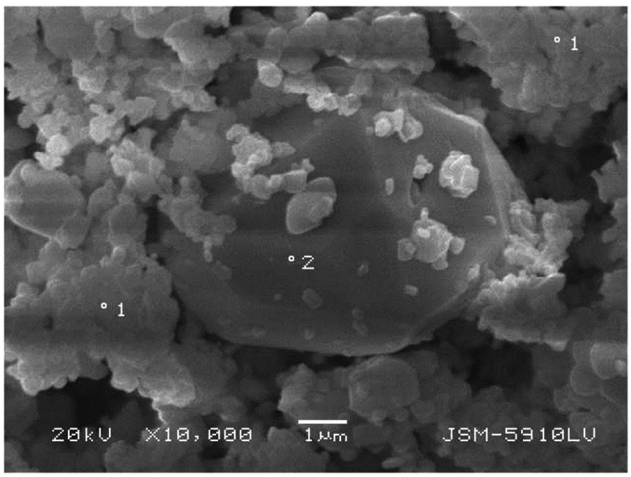

Fig. 7 The SEM picture of the 6 mol% Nd doped $CoNb_2O_6$ columbite powders calcined at 800 °C for 4 hours. Point (1) indicates the single $CoNb_2O_6$ phase and point (2) indicates the secondary $NbNdO_4$ phase.

3.2. Laser induced emission spectra of Nd doped $CoNb_2O_6$ powders

Luminescence measurements of Nd^{3+} doped $CoNb_2O_6$ powders measured upon 805.2 nm excitation contain two bands corresponding to the transitions from the $^4F_{3/2}$ to $^4I_{11/2}$ level. Emission spectra of the laser transition at 1064 nm due to the $^4F_{3/2}\rightarrow{}^4I_{11/2}$ measured at 300 K are shown in Fig. 8.

As it can be clearly seen from the emission spectra in Fig. 8, it was found that the *J*-manifolds of Nd^{3+} ions were split due to the symmetry of $CoNb_2O_6$ cation sites and the spectral profile and the Stark level were the same for the two powders. This behavior can be explained from the fact that the local symmetry of ligand ions surrounding Nd^{3+} ions were the same for the powders. The intensity ratio of 1.6 μm/1.9 μm increased with increasing Nd^{3+} ion concentration. Concentration quenching did not occur for 6.0 mol% Nd^{3+} doped powder.

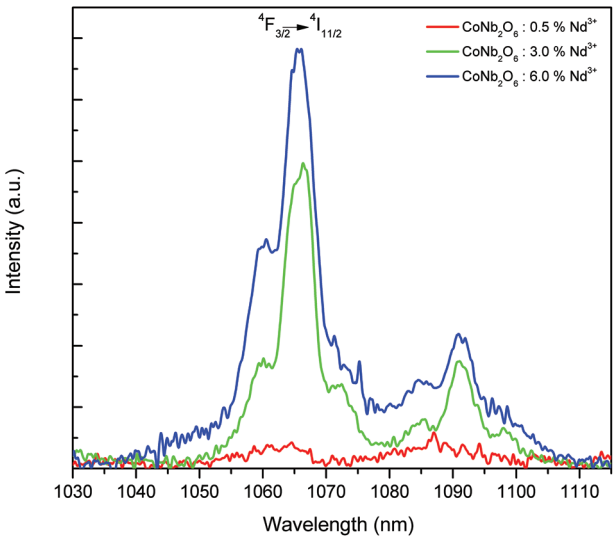

Fig. 8 Emission spectra of the phosphor powders for the $^4F_{3/2}\rightarrow{}^4I_{11/2}$ transition in $CoNb_2O_6$ powders doped with Nd^{3+} at 300 K.

3.3. Xe-flash lamp excited emission spectra of Eu doped $CoNb_2O_6$ powders

Luminescence measurements of Eu^{3+}doped $CoNb_2O_6$ powders were taken between 400 and 700 nm using a Xe-flash lamp, excitation at 395 nm has exhibited a red emission at 615 nm related to the $^5D_0\rightarrow{}^7F_2$ electric dipole transition. Because of the similarity of ionic ratios of Co^{2+} and Eu^{3+} ions (Co^{2+} = 0.88 Å, Eu^{3+} = 0.947 Å),[31] the location of Eu^{3+} dopants has been estimated as non-centrosymmetric CoO_6 octahedral sites that have no inversion symmetry exhibiting the $^5D_0\rightarrow{}^7F_2$ electric dipole transition while the magnetic dipole transition has not been observed at about 590 nm for the Eu^{3+} doped sample in our study.[6–33] Related to these spectral findings, the main possible reasons can be attributed to the crystal field results for the Eu^{3+} doped powders. As the higher Eu^{3+} dopants were incorporated into the pure $CoNb_2O_6$, it led to the formation of a secondary phase and correspondingly, a change in the coulomb attraction force may expose the Eu^{3+} dopant under the influence of different crystal fields, and such a case may lead to the red-shift or blue-shift on the emission spectra. The minor phase $EuNbO_4$ formation would increase the Eu atoms occupying the non-centrosymmetric sites due to the forced electric dipole transition $^5D_0\rightarrow{}^7F_2$ becoming hypersensitive.[28] Depending on the increasing concentration of Eu^{3+} ions from 0.5 to 3.0 mol%, much more ions invade the non-centrosymmetric sites and much more excitation energies absorbed by the CoO_6 groups and then transfer to the dopants showing an increase in the emission intensity. According to the cross-relaxation mechanism, excess of dopant ions might interact and transfer the energy in the decreased ion spacing and lead to the concentration quenching with increasing concentration of Eu^{3+} ions in the host lattice. Consequently, a remarkable decrease has been observed for the 6.0 mol% Eu^{3+} doped sample in the spectra (Fig. 9).[34]

Published on 17 February 2015. Downloaded by Seton Hall University on 05/04/2015 14:27:06.

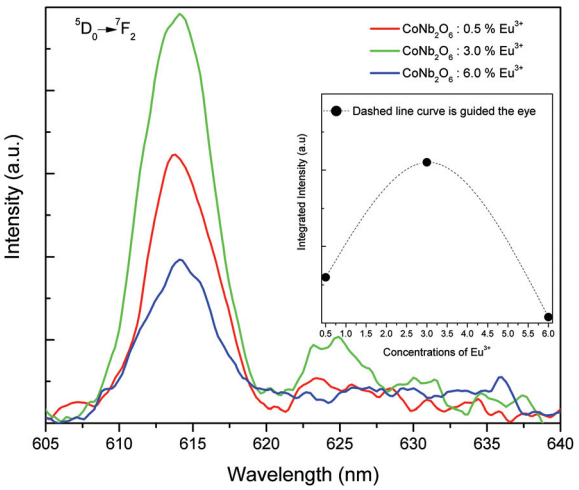

Fig. 9 Emission spectra of the phosphor powders for the $^4D_0 \rightarrow {}^7F_2$ transition in $CoNb_2O_6$ powders doped with Eu^{3+} at 300 K.

4. Conclusion

In this study, the Eu^{3+} or Nd^{3+}-doped $CoNb_2O_6$ powders were successfully synthesized using a molten salt synthesis method. The following results were obtained:

(1) When Nd^{3+} doping concentration was increased from 0.5 to 6.0 mol% the $CoNb_2O_6$ phase remained as a single orthorhombic structure only for the 0.5 mol% doping concentration and beyond this, the $NdNbO_4$ phase started to appear. The emission intensity has increased as the doping concentration increased without any quenching phenomenon.

(2) When the amount of europium ions doped at 0.5 to 3% into the $CoNb_2O_6$ crystalline structure, the emission intensity increased and then decreased to 6.0 mol% due to the excess Eu concentration and so concentration quenching occurred.

Since Nd-doped $CoNb_2O_6$ crystalline powders have shown luminescence in the near-Infrared spectral region at 1064 nm and Eu-doped $CoNb_2O_6$ in the UV-Vis region at 615 nm, it may be a promising phosphor for photonic applications.

Acknowledgements

The authors would like to thank the Marmara University Research Fund (BAPKO) under Project no. FEN-A-150513-0171 for supporting this research.

Notes and references

1 J. H. Sturdivant, The crystal structure of columbite, *Z. Kristallogr.*, 1930, **75**, 88–105.
2 M. K. Ekmekçi, M. Erdem, A. Mergen, G. Özen and B. D. Bartolo, Molten Salt Synthesis and Spectral Properties of Nd^{3+} Doped $CdNb_2O_6$ Columbite Phosphors, *J. Alloys Compd.*, 2014, **591**, 230–233.
3 Y. Zhou, M. Lü, Z. Qiu, A. Zhang, Q. Ma, H. Zhang, G. Zhou and Z. Yang, Photoluminescence characteristics of pure and Dy-doped $ZnNb_2O_6$ nanoparticles prepared by a combustion method, *J. Phys. Chem. C*, 2007, **111**, 10190–10193.
4 R. Zhou, X. Wei, S. Huang, Y. Chen and M. Yin, Efficient near infrared quantum cutting in Yb^{3+} doped $CaNb_2O_6$ phosphor based on energy transfer, *J. Alloys Compd.*, 2012, **537**, 123–126.
5 J. Cao, Y. Ji, J. Li, Z. Zhu, Y. Wang, Z. You and C. Tu, Crystal growth, Judd Ofelt analysis and fluorescence properties of Tm^{3+}: $CaNb_2O_6$ Crystal, *J. Lumin.*, 2011, **131**, 1350–1354.
6 A. S. S. Camargo, R. A. Silva, J. P. Andreeta and L. A. O. Nunes, Stimulated emission and excited state absorption in neodymium-doped $CaNb_2O_6$ single crystal fibers grown by LHPG technique, *Appl. Phys. B: Lasers Opt.*, 2005, **80**, 497–502.
7 A. S. S. Camargo, C. R. Ferrari, R. A. Silva, L. A. O. Nunes, A. C. Hernandes and J. P. Andreeta, Spectroscopic features of erbium-doped $CaNb_2O_6$ (M = Nb,Ta) single crystal fibers grown by laser heated pedestal growth technique, *J. Lumin.*, 2008, **128**, 223–226.
8 D. Prabhakaran, F. R. Wondre and A. T. Boothroyd, Preparation of large single crystals of ANb_2O_6 (A = Ni, Co, Fe, Mn) by the floating-zone method, *J. Cryst. Growth*, 2003, **250**, 72–76.
9 I. S. Mulla, N. Natarajan, A. B. Gaikwad, V. Samuel, U. N. Guptha and V. Ravi, A coprecipitation technique to prepare $CoTa_2O_6$ and $CoNb_2O_6$, *Mater. Lett.*, 2007, **61**, 2127–2129.
10 N. Chaiyo and N. Vittayakorn, Effect of calcination conditions on phase formation of microwave dielectric cobalt niobate ($CoNb_2O_6$) powders via mixed oxide synthesis route, *J. Ceram. Process. Res.*, 2008, **9**, 381–384.
11 S. Kobayashi, S. Mitsuda, M. Ishikawa, K. Miyatani and K. Kohn, *Phys. Rev. B: Condens. Matter*, 1999, **60**, 3331.
12 M. Unruan, N. Vittayakorn, R. W. A. Prasatkhetragarn, S. Ananta and R. Yimnirun, Synthesis and properties of $Pb(Co_{1/3}Nb_{2/3})O_3$ ceramics, *J. Alloys Compd*, 2008, **466**, 264–267.
13 M. Maeda, T. Yamamura and T. Ikeda, Dielectric Characteristics of Several Complex Oxide Ceramics at Microwave Frequencies, *Jpn. J. Appl. Phys., Part 1*, 1987, **26–2**(Suppl.), 76–79.
14 A. Belous, O. Ovchar, B. Jancar and J. Bezjak, The Effect of Non-stoichiometry on the Microstructure and Microwave Dielectric Properties of the Columbites $A^{2+}Nb_2O_6$, *J. Eur. Ceram. Soc.*, 2007, **27**, 2933–2936.
15 A. G. Belous, O. V. Ovchar, A. V. Kramarenko, D. O. Mishchuk, B. Jancar, J. Bezjak and D. Suvorov, Effect of Nonstoichiometry on the Structure and Microwave Dielectric Properties of Cobalt Metaniobate, *Inorg. Mater.*, 2006, **42**, 1369–1373.
16 P. W. C. Sarvezuk, E. J. Kinast, C. V. Colin, M. A. Gusma, J. B. M. da Cunha and O. Isnard, *J. Appl. Phys.*, 2011, **109**, 07E160.

 This journal is © The Royal Society of Chemistry 2015

Published on 17 February 2015. Downloaded by Seton Hall University on 05/04/2015 14:27:06.

17 A. G. Belous, O. V. Ovchar, A. V. Kramarenko, D. O. Mishchuk, B. Jancar, J. Bezjak and D. Suvorov, Effect of Nonstoichiometry on the Structure and Microwave Dielectric Properties of Cobalt Metaniobate, *Inorg. Mater.*, 2006, **42**, 1369–1373.
18 K. H. Yoon, Y. S. Cho, D. H. Lee and D. H. Kang, Powder Characteristics of $Pb(Mg_{1/3}Nb_{2/3})O_3$ Prepared by Molten Salt Synthesis, *J. Am. Ceram. Soc.*, 1993, **76**, 1373–1376.
19 K. H. Yoon, Y. S. Cho and D. H. Kang, Molten Salt Synthesis of Lead-Based Relaxors, *J. Mater. Sci.*, 1998, **33**, 2977–2984.
20 L. Guo, J. Dai, J. Tian, Z. Zhu and T. He, Molten Salt Synthesis of $ZnNb_2O_6$ powder, *Mater. Res. Bull.*, 2007, **42**, 2013–2016.
21 A. A. Kaminskii, *Laser Crystals their Physics and Properties, Springer Series in Optical Sciences*, Springer-Verlag, Berlin, 1981, vol. 14.
22 D. C. Brown, *High-Peak Power Nd:Glass Systems, Springer Series in Optical Sciences*, Springer-Verlag, Berlin, 1981, vol. 25.
23 S. E. Stokowski, in *C R C, Handbook of Laser Science of Technology, Lasers and Masers*, CRC Press, Florida, 1982, vol. 1, p. 215.
24 A. Penzkofer, *Prog. Quant. Electron.*, 1988, **12**, 291.
25 W. Koechner, *Solid-State Laser Engineering, Springer Series in Optical Sciences*, Springer-Verlag, Berlin, 2nd edn, 1988, vol. 1.
26 P. F. Moulton, in *C R C, Handbook of Laser Science and Technology*, CRC Press, Florida, 1982, vol. 21, p. 1.
27 G. Zhu, Z. Ci, C. Ma, Y. Shi and Y. Wang, A novel red emitting phosphor of Eu^{3+} doped TTB-type niobate $NaSr_2Nb_5O_{15}$ for white LEDs, *Mater. Res. Bull.*, 2013, **48**, 1995–1998.
28 T.-H. Fang, Y.-J. Hsiao, Y.-S. Chang and Y.-H. Chang, Photoluminescent Characterization of $KNbO_3:Eu^{3+}$, *Mater. Chem. Phys.*, 2006, **100**, 418–422.
29 A. Belous, O. Ovchar, B. Jancar and J. Bezjak, The effect of non-stoichiometry on the microstructure and microwave Dielectric properties of the columbites $A^{2+}Nb_2O_6$, *J. Eur. Ceram. Soc.*, 2007, **27**, 2933–2936.
30 I. Kashif, A. A. Soliman, E. M. Sakr and A. Ratep, Effect of different conventional melt quenching Technique on Purity of Lithium Niobate ($LiNbO_3$) nano Crystal Phase formed in Lithium Borate Glass, *Results Phys.*, 2012, **2**, 207–211.
31 R. D. Shannon, Revised effective ionic radii and systematic studies of interatomic distances in halides and chalcogenides, *Acta Crystallogr., Sect. A: Cryst. Phys., Diffr., Theor. Gen. Cryst.*, 1976, **32**, 751–767.
32 X. Y. Chen and G. K. Liu, *J. Solid State Chem.*, 2005, **178**, 419.
33 S. Shionoya and W. M. Yen, *Phosphor Handbook*, CRC Press, Boca Raton, 1999.
34 K. N. Shinde, *et al.*, *Phosphate Phosphors for Solid-State Lighting*, 41 Springer Series in Materials Science, Springer-Verlag, Berlin Heidelberg, 2013, p. 174, DOI: 10.1007/978-3-642-34312-4_2.
35 J. Lin, Z. Zhou and Q. Wang, Molten salt synthesis, characterization, and luminescence properties of $GdNbO_4$/$LuTaO_4:Eu^{3+}$phosphors, *Mater. Res. Bull.*, 2013, **48**, 2771–2775.
36 J. Lin, Z. Zhou and Q. Wang, Dibenzoyl-L-cystine as organic directing agent for assembly of visible-light-sensitized luminescent $AgGd(MoO_4)2:Eu^{3+}$ nanowires, *Mater. Res. Bull.*, 2012, **47**, 856–860.
37 S. A. Ghafouri, M. Erdem, M. K. Ekmekçi, A. Mergen and G. Özen, Concentration effect of Er^{3+} ions on structural and spectroscopic properties of CdNb2O6 phosphors, *Mater. Res. Bull.*, 2014, **60**, 562–565.